

6. DISCUSSION

The self-consistent values we find in two iterations are $m_\omega^2 \approx 21.8 m_\pi^2$ and $\gamma_{\omega\rho\pi^2} \approx 2.15/m_\pi^2$. The experimental value of m_ω^2 is $31.4 m_\pi^2$. One can estimate the coupling constant $\gamma_{\omega\rho\pi^2}$ from the decay¹¹ of ω into 3π and the experimental value $\Gamma_\omega \approx 9.5$ MeV.¹² This gives

$\gamma_{\omega\rho\pi^2} \approx 15.4/m_\pi^2$. The agreement is fair enough in high-energy physics.

The curious thing one observes about the computed D function is that it has a second zero at about $S \approx 32.8 m_\pi^2$ with a positive slope. It may simply be due to the inadequate treatment of the π cut while applying unitarity.

¹¹ M. Gell-mann, D. Sharp, and W. G. Wagner, Phys. Rev. Letters **8**, 261 (1962).

¹² N. Gelfand, D. Miller, M. Nussbaum, J. Ratan, J. Schultz, *et al.*, Phys. Rev. Letters **11**, 436 (1963); R. Armenteros, D. N. Edwards, T. Jacobsen, A. Shapira, J. Vandermeulen *et al.*, Proceedings of the Sienna International Conference on elementary particles, 1963 (to be published).

ACKNOWLEDGMENTS

It is a pleasure to thank Dr. L. A. P. Balázs for suggesting the problem and innumerable clarifications, and to Dr. S. N. Biswas, Dr. S. K. Bose and Shri B. M. Udgaonkar who helped by clarifying various points through frequent discussions.

Bound States and Regge Trajectories in a Vector Meson Exchange Model. I. Application to the $K\bar{K}$ System*

RICHARD C. ARNOLD

Department of Physics, University of California at Los Angeles, Los Angeles, California

(Received 10 January 1964)

Partial-wave dispersion relations, extended to noninteger angular momenta are utilized, together with assumptions on the dominance of one-meson exchange to compute the properties of bound states. The exchanged mesons are represented by Regge poles, which lead to a set of equations of generalized Fredholm type when the N/D technique is applied. Bound-state energies in a one-channel system of two spinless particles are computed, as well as the slope of the Regge trajectory which passes through each bound state; the latter is accomplished by an extension of the N/D formalism to angular momenta in the neighborhood of the positive integers. Threshold questions are treated by an approximation for more complex diagrams. The integral equations are solved without further approximations by electronic computer methods. The model is applied to the φ meson as a nearly bound state of the $K\bar{K}$ system in the present work and yields information on S -wave $K\bar{K}$ interactions. Application to future "bootstrap" calculations, the reason for computing the Regge slopes, is discussed, as well as the relationship to the strip approximation.

I. INTRODUCTION

IN this paper we study a simple model strong interaction calculation based on the idea that single-vector meson exchange mechanisms are the dominant dynamical singularities in the analytically continued S matrix. A one-channel elastic scattering amplitude for two nonidentical pseudoscalar particles, satisfying a Mandelstam representation, is chosen for definiteness; it is only a matter of detail based on previous analyses to generalize to particles with spin,¹ multichannel reactions,² and reactions which lead in this model to com-

plex singularities.³ We specialize further to discuss the physical problem of the $K\bar{K}$ amplitude, assuming ρ -meson exchange is the dominant interaction. This has physical interest due to the discovery of the φ meson.⁴ The hypothesis that the φ is a simple elastic P -wave resonance in the $K\bar{K}$ system is examined; and theoretical reasons are put forth, based on the model calculation, that an isoscalar, scalar meson (σ) should exist. It appears in our model as an S -wave bound state of K and \bar{K} .

The main applications of this model, however, are expected to be in "bootstrap" calculations in which the

* This work partially supported by the National Science Foundation.

¹ For the spin- $\frac{1}{2}$ -spin- $\frac{1}{2}$ problem see for example M. L. Goldberger, M. T. Grisaru, S. W. MacDowell, and D. Y. Wong, Phys. Rev. **120**, 2250 (1960); B. R. Desai and R. G. Newton, *ibid.* **129**, 1437 (1963). For spin- $\frac{1}{2}$ -spin-0 scattering, cf. S. C. Frautschi and J. D. Walecka, Phys. Rev. **120**, 1486 (1960); V. Singh, *ibid.* **129**, 1889 (1963).

² J. Bjorken, Phys. Rev. Letters **4**, 473 (1960); J. Bjorken and M. Nauenberg, Phys. Rev. **121**, 1250 (1961); R. Blankenbecler, *ibid.* **122**, 983 (1961); J. M. Charap and E. J. Squires, Ann. Phys. (N. Y.) **21**, 8 (1963).

³ L. F. Cook and B. W. Lee, Phys. Rev. **127**, 283 (1962); J. S. Ball, W. R. Frazer, and M. Nauenberg, *ibid.* **128**, 478 (1962); J. M. Cornwall, K. T. Mahanthappa, and V. Singh, *ibid.* **131**, 1882 (1963).

⁴ N. Gelfand, D. Miller, M. Nussbaum, J. Ratan, J. Schultz, J. Steinberger, and T. Tau, Phys. Rev. Letters **11**, 438 (1963); P. Schlein, W. Slater, L. Smith, D. H. Stork, and H. Ticho, Phys. Rev. Letters **10**, 368 (1963); P. L. Connolly, E. L. Hart, K. W. Lai, G. London, G. C. Monati *et al.*, Phys. Rev. Letters **10**, 371 (1963); L. Bertanza, V. Brisson, P. L. Connolly, E. L. Hart, I. S. Mitra *et al.*, Phys. Rev. Letters **9**, 180 (1962).

exchanged vector meson is itself produced as a $J=1$ bound state, thus forming a self-consistent system. (It should be emphasized that the calculation as presented in this paper is *not* a bootstrap calculation since we do not assume the ρ is a bound state of K and \bar{K} .) Such physical models have been investigated by many authors^{5,6} since Chew and Mandelstam⁷ originally proposed such a situation for the π - π amplitude. Most of these investigations, however, have been hampered by a lack of a good prescription for analytical continuation. Specifically, one needs to continue the amplitude representing the meson as a pole in the energy variable, where it appears as the result of a partial-wave calculation, into the unphysical region corresponding to the exchange of the meson, where it appears as a dynamical singularity in the crossed channel. One cannot use the partial-wave decomposition directly, since the Legendre series diverges when the physical roles of energy and momentum transfer are interchanged. This problem was clarified by the use of the Sommerfeld-Watson transform in potential theory,⁸ leading to the recognition that resonances and bound states may be fruitfully represented by poles in the complex angular momentum plane.⁹

This representation, and its relation to the double-dispersion (Mandelstam) representation, were discussed by Chew, Frautschi, and Mandelstam,¹⁰ and some of the consequences for bootstrap calculations were exploited first by Wong.⁵ The latter utilized the structure of the Regge pole term associated with the ρ meson to carry out a calculation of the $\pi\pi\rho$ bootstrap, with the slope (α') of the Regge trajectory associated with the ρ introduced as an input parameter. This parameter was varied, and the character of the bootstrap solutions was found to limit the possible values which one could assume for α' . In this sense, α' replaced the older cutoff parameters or subtraction prescriptions which had been introduced previously in an *ad hoc* fashion¹¹ to get solutions to the partial-wave dispersion relations when vector-meson exchanges were considered. Such semi-phenomenological Regge behavior has been used in describing nucleon-nucleon scattering with vector meson exchange, with considerable success.¹²

If one is to carry out a calculation in the bootstrap philosophy, however, one is faced with the difficulty that the Regge slope α' associated with the vector meson (or resonant state) should be deduced from the *results* of the calculation, in order that a self-consistent model is achieved. Only if this is done can we hope to eliminate arbitrary parameters and see the true consequences of bootstrap-model assumptions.

There has been proposed one method¹³ for explicitly calculating the trajectory functions $\alpha(S)$ which may be applicable to the self-consistent S -matrix approach, but at the present state difficulties have been encountered with applying the method outside of potential theory. Furthermore, the integral equations involved are quite nonlinear and are not immediately susceptible to classical methods of analysis, which makes it difficult to examine the existence and uniqueness of solutions for the equations, even in approximate form.

In the present work we seek to avoid unnecessary complications by using partial-wave dispersion relations to compute one additional parameter α' , which is sufficient for completing a bootstrap calculation. Here α' is defined to be the slope of the Regge trajectory which passes through the bound state or resonance of angular momentum l , evaluated at the point where $\alpha(S)=l$. If we assume that this slope is small and that we can extrapolate to $S=0$ with reasonable accuracy, then the asymptotic behavior of the partial-wave amplitudes in the crossed channels is determined as a function of α' . This asymptotic behavior yields a convergent set of (generalized) partial-wave dispersion relation source terms, and an iterative procedure is made possible with no *ad hoc* convergence parameters necessary.

The computation is carried out explicitly for the case of ρ exchange in the $T=0$ state of $K\bar{K}$ elastic scattering, as mentioned above. No attempt at a bootstrap is made. It is apparent that in reality besides ρ exchange, we will have ω and φ vector meson exchanges as well as (possibly) scalar meson exchanges. The calculation done here assumes that for the $T=0$ state, the other two vector mesons have a contribution which can be lumped with the ρ term. The coupling constant $f_{\rho K K^2}$ which we investigate should thus be understood as representing an effective sum over ρ , ω , and φ exchange terms. Explicit inclusion of the separate terms is a trivial matter, formally, and is not done here because we want to simplify the presentation.

There is some additional physical inconsistency in the model calculation done here. We have ignored the p -wave amplitude poles in the direct (S) channel corresponding to ω (in the $T=0$ state) and ρ (in the $T=1$ state). The point of the present calculation is to exhibit the bound-state properties as they depend on the *exchange* of a vector meson, corresponding to the studies

⁵ Some examples are F. Zachariasen, Phys. Rev. Letters **7**, 112 (1961) and **7**, 268 (1961); D. Y. Wong, Phys. Rev. **126**, 1220 (1962); R. H. Capps, Phys. Rev. **131**, 1307 (1963); R. E. Cutkosky, Ann. Phys. (N. Y.) **23**, 415 (1963); F. Zachariasen and C. Zemach, Phys. Rev. **128**, 849 (1963).

⁶ I. M. Barbour and K. Nishimura, Nuovo Cimento **29**, 288 (1963).

⁷ G. F. Chew and S. Mandelstam, Phys. Rev. **119**, 467 (1960); Nuovo Cimento **19**, 752 (1961).

⁸ T. Regge, Nuovo Cimento **14**, 951 (1959); **18**, 947 (1960); A. Bottino, A. M. Longani, and T. Regge, *ibid.* **23**, 954 (1962).

⁹ R. Blankenbecler and M. L. Goldberger, Phys. Rev. **126**, 766 (1962).

¹⁰ G. F. Chew, S. C. Frautschi, and S. Mandelstam, Phys. Rev. **126**, 1202 (1962).

¹¹ See, for example, F. Zachariasen, Ref. 5; R. C. Arnold and J. J. Sakurai, Phys. Rev. **128**, 2808 (1962).

¹² A. Scotti and D. Y. Wong, Phys. Rev. Letters **10**, 142 (1963).

¹³ H. Cheng and D. Sharp, Ann. Phys. (N. Y.) **22**, 481 (1963); S. C. Frautschi, P. E. Kaus, and F. Zachariasen, Phys. Rev. **133**, B1607 (1964).

which have been carried out in potential scattering. The inclusion of the poles mentioned above could affect the numerical results of the actual $K\bar{K}$ system scattering amplitude substantially, but we do not wish to emphasize the connection with experiment. In a bootstrap calculation, which is the design purpose of the method, such direct poles would not exist separately from the bound states obtained from the calculation; e.g., if we assumed only φ meson exchange in the present model we would be in the bootstrap spirit, and the question of ρ and ω poles would not exist.

It is believed by the author that the worst feature of the model in the $K\bar{K}$ problem is the restriction to a one-channel calculation. It would clearly be of interest to enlarge the dimensionality of the amplitude to include π and η mesons as well as $K\bar{K}$; but physically realistic results may only come about when the $N\bar{N}$ channels are included. This applies in particular to the φ meson, since it is believed to have some intimate dynamical connection with the ω ; the latter has been thought a good candidate for a bound state of nucleon and antinucleon through a bootstrap process. This will be discussed further in Sec. VI.

II. FORMULATION OF BASIC EQUATIONS; S-WAVE STATES

Assuming that we represent the ρ meson as a $J=1$ Regge pole in the channel for $K\bar{K}$ scattering, we have¹⁰ for this pole contribution to the scattering amplitude the expression

$$T_\rho(t, S) = (2\alpha + 1) \times \frac{-\beta(t)}{\sin\pi\alpha(t)} P_{\alpha(t)}[-1 - 2S/(t - 4M_K^2)]. \quad (2.1)$$

Here $t \geq 4M_K^2$, S is the negative of the momentum transfer squared, and $\alpha(t) \equiv \alpha_\rho(t)$ and $\beta(t) \equiv \beta_\rho(t)$ are the Regge trajectory and residue functions associated with the ρ meson. We know that $\alpha(M_\rho^2) = 1$, and $\beta(M_\rho^2)$ is proportional to the square of the $KK\rho$ coupling constant. To reduce the number of input parameters, we seek to approximate this pole term by evaluating functions wherever possible at the pole position, $t = M_\rho^2$. The extent to which this is justified has not been rigorously established; we must be guided by a correspondence with the expression for an elementary vector meson¹⁴ from perturbation theory. The expression deduced from simplification of the above term must be only a slight modification of the elementary case when α is close to unity for all t . This leads to replacement of t in the argument of the Legendre function by M_ρ^2 , and similarly replacement of $\beta(t)/\sin\pi\alpha(t)$ by a simple pole in t , e.g., $-f_\rho^2/(M_\rho^2 - t)$. The arguments of Wong⁵ may be applied to this point. [The value of f_ρ^2 may also be

determined by correspondence in terms of $(M_\rho^2 - 4M_K^2)$ and $f_{\rho KK^2}$, but that is not required at this point.] The replacement of $(2\alpha + 1)$ by 3 is optional, since we are going to assume that α_ρ departs only slightly from unity wherever the contribution from T_ρ is large.

Finally, we write the resulting term down and relabel it as $B_\rho(t, S)$;

$$B_\rho(t, S) = \frac{3f_\rho^2}{M_\rho^2 - t} P_{\alpha(t)}[-1 - 2S/(M_\rho^2 - 4M_K^2)]. \quad (2.2)$$

Now using crossing relations, we consider this as the pole approximation for $K\bar{K}$ scattering in S channel, by considering $t \leq 0$ and $S \geq 4M_K^2$. We see that for $S \geq 4M_K^2$, there is no branch point of this function, which means we can take this as it stands as the source of the left-hand cut in the partial-wave amplitudes of the S channel. We thus do not encounter the problems discussed (e.g., by Chew¹⁵) in subtracting out a part of the Regge-pole associated spectral function to achieve the appropriate analyticity properties.

The Regge-type representation of Khuri¹⁶ might be a better starting point than (2.1) for development of our model, but the form (2.1) was chosen to simplify numerical computations. It is believed that no appreciable difference would result in the calculation we have carried out if (2.1) had been replaced by the corresponding Khuri pole. It might be prudent to do this in other situations, however, and Chew has proposed such a starting point in the new version of the strip approximation.¹⁵ We shall need the representation of B_ρ in the angular momentum variable λ for the S channel; we must choose the continuation of the scattering amplitudes $T_t(S)$ to complex angular momenta λ in accordance with the prescription of Froissart¹⁷ if we are to utilize the result for noninteger values of λ . It has been shown¹⁵ that an equivalent representation of the scattering amplitude for complex λ is given by

$$T_\lambda(S) = \frac{1}{2} \int_{-1}^{+1} dZ P_\lambda(Z) T(t, S) - \frac{\sin\pi\lambda}{\pi} \int_{-\infty}^{-1} dZ Q_\lambda(-Z) T(t, S), \quad (2.3)$$

where $T(t, S)$ is the scattering amplitude expressed in the variables $S = W^2$ and $t = -2k^2(1 - Z)$.

Thus, in terms of the angular momentum variable λ , the one-Regge-pole contribution to the S -channel $K\bar{K}$

¹⁴ M. Gell-Mann and F. Zachariasen, Phys. Rev. **124**, 953 (1961).

¹⁵ G. F. Chew, Phys. Rev. **129**, 2363 (1963).

¹⁶ N. N. Khuri, Phys. Rev. **130**, 429 (1963).

¹⁷ M. Froissart, Phys. Rev. **123**, 1953 (1961).

scattering amplitude is given by

$$T_\lambda^{(\rho)}(S) = 3f_\rho^2 \left\{ \frac{1}{2} \int_{-1}^{+1} dZ P_\lambda(Z) \right. \\ \times \frac{P_{\alpha(t)}(2S/(4M_K^2 - M_\rho^2) - 1)}{M_\rho^2 - t} \\ - \frac{\sin \pi \lambda}{\pi} \int_{-\infty}^{-1} dZ Q_\lambda(-Z) \\ \left. \times \frac{P_{\alpha(t)}(2S/(4M_K^2 - M_\rho^2) - 1)}{M_\rho^2 - t} \right\}, \quad (2.4)$$

where in each integral $\alpha = \alpha_\rho(t)$, $t = -2k^2(1-Z)$, $k^2 = (S - 4M_K^2)/4$.

We now utilize the N/D method⁷ to write the integral equations which determine the amplitude $T_\lambda(S)$ in such a manner as to insure exact (elastic) unitarity for $S \geq 4M_K^2$, and to coincide with the Regge-pole approximation in the left-hand S plane (on the unphysical or dynamical cuts); and in the high-energy region ($S \rightarrow \infty$) we desire $T_\lambda(S) \rightarrow T_\lambda^{(\rho)}(S)$. The latter follows automatically if we exchange a vector meson such as ρ , and normalize the D function to unity for large $|S|$ values, as will be shown later.

The N/D decomposition for integer $\lambda = l$ depends on the nonoverlapping of cuts along the real S axis in the partial-wave amplitudes $T_l(S)$. We know, however, that for general λ , the amplitudes $T_\lambda(S)$ have a kinematic branch cut¹⁸ from $S = -\infty$ to $S = 4M^2$ which joins up with the unitarity branch cut from $S = 4M^2$ to $S = +\infty$. Thus, before applying the formalism, we must define a new function $\tilde{T}_\lambda(S)$ in such a way that $\tilde{T}_\lambda(S)$ has no cut in some interval. This can be accomplished^{18,19} by writing

$$T_\lambda(S) = (S - 4M_K^2)^\lambda \tilde{T}_\lambda(S). \quad (2.5)$$

Then it can be shown that $\tilde{T}_\lambda(S)$ has only the cuts of the usual partial-wave amplitudes $T_l(S)$; and we can write

$$\tilde{T}_\lambda(S) = N_\lambda(S)/D_\lambda(S), \quad (2.6)$$

where $N_\lambda(S)$ is analytic in a neighborhood of the real S axis from $4M_K^2$ to ∞ , while $D_\lambda(S)$ has as its only singularity a branch cut along the interval $S = 4M_K^2$ to $S = +\infty$. Following the derivation as in the integer λ case,⁷ we can derive integral equations for N_λ and D_λ . Let us define

$$B_\lambda(S) = (S - 4M_K^2)^{-\lambda} T_\lambda^{(\rho)}(S). \quad (2.7)$$

Then the discontinuity of $\tilde{T}_\lambda(S)$ will coincide with the discontinuity of $B_\lambda(S)$ along the dynamical left-hand cuts, and utilizing the unitarity relation for \tilde{T}_λ in

the form

$$(2i)^{-1} [\tilde{T}_\lambda(S+i\epsilon) - \tilde{T}_\lambda(S-i\epsilon)] \\ = (S - 4M_K^2)^\lambda \tilde{T}_\lambda(S+i\epsilon) \tilde{T}_\lambda(S-i\epsilon) \rho(S),$$

we can derive the following integral equation²⁰ for $N_\lambda(S)$;

$$N_\lambda(S) = B_\lambda(S) + \frac{1}{\pi} \int_{4M_K^2}^{\infty} dS' \rho(S') (S' - 4M_K^2)^\lambda \\ \times \left[\frac{B_\lambda(S) - B_\lambda(S')}{S - S'} \right] N_\lambda(S'). \quad (2.8)$$

Here $\rho(S) = [(S - 4M_K^2)/S]^{1/2}$. The denominator function is then given by

$$D_\lambda(S) = 1 - \frac{1}{\pi} \int_{4M_K^2}^{\infty} dS' \frac{\rho(S') (S' - 4M_K^2)^\lambda N_\lambda(S')}{S' - S}. \quad (2.9)$$

According to the results of Mandelstam,¹⁹ these equations hold at least for all complex λ such that $|\text{Re} \lambda|$ is sufficiently small.

Now the Regge poles will be given by the zeros of $D_\lambda(S)$ when $S < 4M_K^2$, and approximately by the zeros of $\text{Re} D_\lambda(S)$ for $S > 4M_K^2$, at least if the trajectory passes by the integers with small imaginary part. Since we will be concerned with bound states ($S < 4M_K^2$) or very low-energy resonances in the $K\bar{K}$ problem, we simply assume that every zero of $\text{Re} D_\lambda(S)$ represents a Regge pole. With this in mind, we can identify the physical S and P wave bound states and resonances by solving the integral equation (2.8) for $\lambda = l$, $l = 0, 1$; then locating S values S_B such that $\text{Re} D_l(S_B) = 0$. We can identify these points as intersections of Regge trajectories with the integers 0 and 1. In the neighborhood of such intersections, we can write the constraint satisfied by the trajectory $\alpha_B(S)$ for small changes in S as

$$(\Delta \alpha_B) \frac{\partial D_\lambda(S_B)}{\partial \lambda} \Big|_{\lambda=l} + (\Delta S) \frac{\partial D_l(S)}{\partial S} \Big|_{S=S_B} = 0. \quad (2.10)$$

This means we can compute the slope $d\alpha_B(S)/dS$, evaluated at the position of a physical bound state, as

$$\alpha_B'(S_B) = -(\partial D_l(S)/\partial S)_{S_B} / (\partial D_\lambda(S_B)/\partial \lambda)_l, \quad (2.11)$$

where l is the angular momentum of the bound state. The numerator of this expression is trivially computed from the solution of Eq. (2.8) for integer λ , as in previous calculations. The denominator in expression (2.11), however, requires the solution of an equation slightly more complicated than in the integer case, although somewhat simpler than the Eq. (2.8) for arbitrary λ . Starting from the expression (2.9), we take the deriva-

¹⁸ K. Bardacki, Phys. Rev. **127**, 1832 (1962); **130**, 369 (1963). [Note that the present work has very little relation to the procedure suggested in the latter paper.]

¹⁹ S. Mandelstam, Ann. Phys. (N. Y.) **21**, 302 (1963).

²⁰ J. L. Uretsky, Phys. Rev. **123**, 1459 (1961).

tive with respect to λ and evaluate at $\lambda=l$;

$$\left. \frac{\partial D_\lambda(S)}{\partial \lambda} \right|_{\lambda=l} = -\frac{1}{\pi} \int_{4M_K^2}^{\infty} dS' \rho(S') (S' - 4M_K^2)^l \times \left[\ln(S' - 4M_K^2) N_l(S') + \left. \frac{\partial N_\lambda(S')}{\partial \lambda} \right|_{\lambda=l} \right]. \quad (2.12)$$

Now let

$$E_l(S) \equiv \left. \frac{\partial N_\lambda(S)}{\partial \lambda} \right|_{\lambda=l}, \quad \text{and} \quad F_l(S) = \left. \frac{\partial B_\lambda(S)}{\partial \lambda} \right|_{\lambda=l}.$$

From Eq. (2.18), taking the derivative with respect to λ yields

$$E_l(S) = F_l(S) + \frac{1}{\pi} \int_{4M_K^2}^{\infty} dS' \rho(S') (S' - 4M_K^2)^l \times \left[\ln(S' - 4M_K^2) \frac{B_l(S) - B_l(S')}{S - S'} + \frac{F_l(S) - F_l(S')}{S - S'} \right] N_l(S') + \frac{1}{\pi} \int_{4M_K^2}^{\infty} dS' \rho(S') \times (S' - 4M_K^2)^l \left[\frac{B_l(S) - B_l(S')}{S - S'} \right] E_l(S'). \quad (2.13)$$

Given $F_l(S)$, $B_l(S)$, and $N_l(S)$ as the solution of Eq. (2.18), this becomes an integral equation for the determination of $E_l(S)$. Note that this equation has exactly the same kernel as Eq. (2.8), but a different inhomogeneous term,

$$G_l(S) \equiv F_l(S) + \frac{1}{\pi} \int_{4M_K^2}^{\infty} dS' \rho(S') (S' - 4M_K^2)^l \times \left[\ln(S' - 4M_K^2) \frac{B_l(S) - B_l(S')}{S - S'} + \frac{F_l(S) - F_l(S')}{S - S'} \right] N_l(S'). \quad (2.14)$$

From (2.7) and (2.4) we obtain

$$F_l(S) = -\ln(S - 4M_K^2) B_l(S) + 3f_\rho^2 \left[\frac{1}{2} \int_{-1}^{+1} dZ \left[\frac{\partial P_\lambda(Z)}{\partial \lambda} \right]_{\lambda=l} \right] \times \frac{P_{\alpha(t)}(2S/(4M_K^2 - M_\rho^2) - 1)}{M_\rho^2 - t} + (-1)^{l+1} \int_{-\infty}^{-1} dZ Q_l(-Z) \times \frac{P_{\alpha(t)}(2S/(4M_K^2 - M_\rho^2) - 1)}{M_\rho^2 - t}. \quad (2.15)$$

Now we have the method for computing $\alpha_B'(S_B)$; first we solve (2.8) for integer λ . This involves the Born term $B_l(S)$, which is the usual partial-wave projection applied to the form (2.4). Then, using this solution $N_l(S)$ and computing $G_l(S)$ from (2.14) and (2.15), we solve (2.13), which can be written as

$$E_l(S) = G_l(S) + \frac{1}{\pi} \int_{4M_K^2}^{\infty} dS' \rho(S') \times \left[\frac{B_l(S) - B_l(S')}{S - S'} \right] (S' - 4M_K^2)^l E_l(S). \quad (2.16)$$

This can be done utilizing the resolvent kernel as found for (2.8). Finally, we use (2.12) to compute the denominator for (2.11), and take the numerator of (2.11) from the integer $-\lambda$ solution found first.

It can be shown¹⁹ from the expression (2.4) that the kernel in (2.8) for $l=0$ is of generalized Fredholm type,²¹ and thus that our S -wave solutions exist and are unique, provided $\alpha_\rho(0) < 1$. This concludes the formal statement of the model as it concerns S -wave bound states. The P -waves, however, require further investigations, and are discussed in the next section.

III. P-WAVE BOUND STATES

If we investigate the asymptotic behavior in our model of the integrands in Eqs. (2.8) and (2.9), it can be shown that the kernel of (2.8) fails to be of generalized Fredholm type when $\text{Re} \lambda \geq 1$.²² This is a consequence of the asymptotic behavior of our one-Regge-pole choice for B_λ . We must find a method for continuing the solutions in λ at least up to $\lambda = 1 + \epsilon$ (ϵ positive) to get the P -wave bound states and slopes since otherwise the derivative of the solution N_λ with respect to λ does not exist at $\lambda = 1$, and this derivative is required for the slope determination. This may be done by a device similar to that used by Mandelstam.¹⁹ Define, for each positive integer n ,

$$\tilde{T}_\lambda^{(n)}(S) = (S - 4M_K^2)^{-n} N_\lambda^{(n)}(S) / D_\lambda^{(n)}(S), \quad (3.1)$$

where

$$D_\lambda^{(n)}(S) = 1 - \frac{1}{\pi} \int_{4M_K^2}^{\infty} \frac{dS' \rho(S') (S' - 4M_K^2)^{\lambda-n}}{S' - S} \times N_\lambda^{(n)}(S'), \quad (3.2)$$

and $N_\lambda^{(n)}$ is the solution of

$$N_\lambda^{(n)}(S) = B_\lambda^{(n)}(S) + \frac{1}{\pi} \int_{4M_K^2}^{\infty} dS' \rho(S') (S' - 4M_K^2)^{\lambda-n} \times \left[\frac{B_\lambda^{(n)}(S) - B_\lambda^{(n)}(S')}{S - S'} \right], \quad (3.3)$$

²¹ F. Smithies, *Integral Equations* (Cambridge University Press, New York, 1958).

²² cf. R. Omnes, Lawrence Radiation Laboratory Report UCRL 11008, 1963, Phys. Rev. **133**, B1543 (1964).

where $B_\lambda^{(n)}$ is defined by

$$B_\lambda^{(n)}(S) = (S - 4M_K^2)^n B_\lambda(S). \quad (3.4)$$

Now it may be shown by the same method as used by Mandelstam¹⁹ that if the dynamical term B_λ is obtained from double spectral functions constructed in the elastic unitarity approximation, then the regions of definition in λ of successive $\tilde{T}_\lambda^{(n)}(S)$ overlap, for $n=0, 1, 2, 3, \dots$, and they are analytic continuations of each other with respect to λ . Thus, they define a function $\tilde{T}_\lambda(S)$ which coincides with the previous representation for small $\text{Re}\lambda$.

The reader must be referred to the discussion in Ref. 19 for the proof, since it is rather lengthy. It is clear that in the limit of small coupling constant, $\tilde{T}_\lambda^{(n)}(S) \rightarrow B_\lambda(S)$ for any n . Of course, in the model calculation here, we do not construct the double spectral functions and then project out B_λ , but rather take B_λ as approximately given by the expression (2.7). It is the author's viewpoint that such an approach is a good starting point and should be modified only by adding further contributions which represent the parts of the double spectral functions implicitly ignored by using the approximation (2.7).

The equations for $n=0$ coincide with the equations of the previous section, and as before, the correct threshold behavior $(S - 4M_K^2)^\lambda$ for the amplitude $T_\lambda(S)$ is maintained for all λ in the interval $(0, 1 - \epsilon)$ when the $n=0$ representation is used. When we change to a representation with $n \geq 1$ it is no longer true that the threshold condition is automatically satisfied; this will be discussed later.

The formulation of the equations presented here, in particular the normalization of D to unity at $S = \infty$, was chosen to follow the approach of Ref. 19 as closely as possible.

We do not consider here the question of the lower limit to which we can analytically continue N_λ and D_λ , except to note that it is at least $\text{Re}\lambda = -\frac{3}{2}$, since our model satisfies the boundedness condition of Mandelstam.¹⁹

Our amplitudes for λ in the neighborhood of 1, which will give the P -wave bound states and slopes, are then represented by putting $n=1$ in (3.1), (3.2), (3.3), and (3.4). The equations for determining the P -wave bound-state location are obtained by putting $\lambda=1$; we get

$$D_1(S) = 1 - \frac{1}{\pi} \int_{4M_K^2}^{\infty} dS' \frac{\rho(S') N_1(S')}{S' - S}, \quad (3.5)$$

where N_1 satisfies

$$N_1(S) = B_1(S) + \frac{1}{\pi} \int_{4M_K^2}^{\infty} dS' \rho(S') \times \frac{B_1(S) - B_1(S')}{S - S'} N_1(S') \quad (3.6)$$

and B_1 is given in our model by

$$B_1(S) = T_1^{(\rho)}(S). \quad (3.7)$$

For the slope equations, we put $n=1$ in (3.2)–(3.4), take the derivative with respect to λ , and set $\lambda=1$ at the end. The resulting equations are

$$\left. \frac{\partial D_\lambda(S)}{\partial \lambda} \right|_{\lambda=1} = -\frac{1}{\pi} \int_{4M_K^2}^{\infty} \frac{dS' \rho(S')}{S' - S} \times \left[\ln(S' - 4M_K^2) N_1(S') + \left. \frac{\partial N_\lambda(S')}{\partial \lambda} \right|_{\lambda=1} \right]. \quad (3.8)$$

Defining E_l, F_l , and G_l as in the preceding section, we find E_1 satisfies

$$E_1(S) = G_1(S) + \frac{1}{\pi} \int_{4M_K^2}^{\infty} dS' \rho(S') \times \left[\frac{B_1(S) - B_1(S')}{S - S'} \right] E_1(S'), \quad (3.9)$$

where G_1 is given by

$$G_1(S) = F_1(S) + \frac{1}{\pi} \int_{4M_K^2}^{\infty} dS' \rho(S') \left[\ln(S' - 4M_K^2) \times \frac{B_1(S) - B_1(S')}{S - S'} + \frac{F_1(S) - F_1(S')}{S - S'} \right] N_1(S') \quad (3.10)$$

and F_1 is, in our model

$$F_1(S) = -\ln(S - 4M_K^2) B_1(S) + 3f_\rho^2 \left\{ \frac{1}{2} \int_{-1}^{+1} dZ \left[\left. \frac{\partial P_\lambda(Z)}{\partial \lambda} \right]_{\lambda=1} \times \frac{P_{\alpha(t)}(2S/(4M_K^2 - M_\rho^2) - 1)}{M_\rho^2 - t} + \int_{-\infty}^{-1} dZ Q_1(-Z) \times \frac{P_{\alpha(t)}(2S/(4M_K^2 - M_\rho^2) - 1)}{M_\rho^2 - t} \right\}. \quad (3.11)$$

The term B_1 here, as in the preceding discussion, is understood (at the moment) to be partial-wave projection of our assumed Regge pole term

$$B_1(S) = \frac{1}{2} \int_{-1}^{+1} dZ P_1(Z) \times \left[3f_\rho^2 \frac{P_{\alpha(t)}(2S/(4M_K^2 - M_\rho^2) - 1)}{M_\rho^2 - t} \right]. \quad (3.12)$$

These equations are then guaranteed to give us, within the framework of the model, the correct slope of

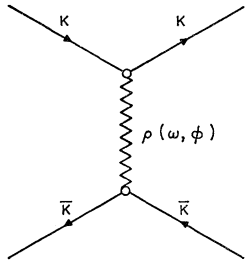


FIG. 1. Basic interaction assumed in model.

the Regge trajectory passing through a P -wave bound state, if any exists, by using the formula (2.11).

However, we now encounter one serious difficulty with using only the term (2.4) to generate the dynamical singularities; it cannot give the correct threshold behavior for $\tilde{T}_l(S)$ when $l \neq 0$. In the S -wave case, we could ignore such questions, but if we are looking for bound P -wave states (or resonances which are close to threshold, like the φ meson), the proper behavior of $N_l(S)$ as $S \rightarrow 4M_K^2$ is essential. In previous calculations, this difficulty has been treated by introducing a phenomenological pole in $B_l(S)$, far away on the negative S axis, and its residue adjusted such that $N_l(S) = \mathcal{O}(S - 4M_K^2)^l$ at threshold. [Writing dispersion relations for the function $T_l(S)[(S + S_1)/(S - 4M_K^2)]^l$ is equivalent to this procedure.] Alternatively, one may simply write a dispersion relation for $T_l(S)(S - 4M_K^2)^{-l}$, as we did in the previous section, but then one encounters the divergence at high S values mentioned above. This is done by Chew,¹⁵ who compensates by cutting off the range of integration at a finite value; but that is not consistent with our approach here.

We cannot introduce a phenomenological pole in B_λ , however, because the residue would be an undetermined function of λ ; this would ruin the computation of the Regge trajectories, in particular the slope equations which we use. Thus, it is necessary to develop some means of correcting the threshold behavior, at least in the P -wave bound-state equation, which enables us to estimate the effect of the added term on the slope of the Regge trajectory and on the S waves, i.e., which involves only known functions of λ .

Now if the complete Mandelstam iterative method²³ were used (starting with the diagram of Fig. 1) to generate the elastic part of the double spectral functions, we know that the threshold behavior would be correct for all partial waves in the final solution $\tilde{T}_\lambda(S)$. This means that if we are to adjust the threshold behavior, the most logical procedure based on the physics of our model would be to add a term which represents the next-higher mass states as they appear on the dynamical cuts of $\tilde{T}_\lambda(S)$. These could come from the left-hand cuts of the crossed and uncrossed fourth-order diagrams, shown in Fig. 2.

To accomplish just this it would be necessary to

²³ S. Mandelstam, Phys. Rev. **112**, 1344 (1958); G. F. Chew and S. C. Frautschi, *ibid.* **123**, 1478 (1962).

compute the amplitudes represented by Fig. 2, where the exchanged "particles" were treated as pairs of Regge poles in the four-particle exchange contribution. To avoid such a complicated function, we will simplify the situation slightly by replacing the exchanged "particles" by scalar mesons (S) which have the same mass as the ρ (vector) meson pole exhibits, M_ρ . Then the contributions of Fig. 2 are easily computed.²⁴ The coupling constants are left arbitrary, and the left-hand cuts from these diagrams are added to the left-hand cut from $\tilde{T}_\lambda^{(\rho)}(S)$. The resulting function for $B_\lambda(S)$ is used in the equations which have already been written down; then for $\lambda = 1$, the coupling constant for the scalar meson S introduced above is adjusted so as to yield the correct threshold behavior for $N_1(S)$. Explicitly, if g is the scalar-meson coupling constant and M_S its mass, the additional term for $B_J(S)$ is given (up to a constant) for integer J by

$$B_J^{(4)}(S) = \frac{g^4}{\pi} \int_{4M_S^2}^{\infty} dt (t - 4M_K^2)^{1/2} \times \int_{t-4M_K^2}^{\infty} dy \frac{P_J[1 - 2t/(y + 4M_K^2)]}{(y + S)(y + 4M_K^2)} \times [f_u(y, t) + f_c(y, t)], \quad (3.13)$$

where f_u, f_c are from the uncrossed and crossed diagrams, respectively, and are given by

$$f_u(y, t) = \frac{1 \coth^{-1}[(t - 4M_S^2)^{1/2}/(\Delta_u/y)^{1/2}]}{y (\Delta_u/y)^{1/2}} \quad (3.14a)$$

and

$$f_c(y, t) = \frac{1 \coth^{-1}[(t - 4M_S^2)^{1/2}/(\Delta_c/Z)^{1/2}]}{Z (\Delta_c/Z)^{1/2}}, \quad (3.14b)$$

where we have written

$$Z = 4M_K^2 + y - t, \quad \Delta_u = yt + 4M_K^2t + 4M_S^2,$$

and

$$\Delta_c = t^2 - yt + 4M_S^2.$$

It is assumed that the exact form of $B_J^{(4)}(S)$ does not

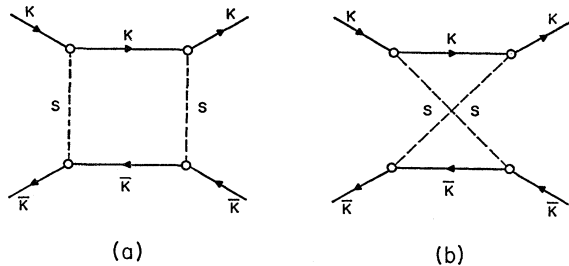


FIG. 2. Higher mass contributions to dynamical singularities.

²⁴ See for example Ref. 1 where the required Feynman integrals are reduced to elementary functions.

critically affect our final results. The general properties we need to know are as follows: (a) $B_J^{(4)}(S)$ is nonzero and slowly varying for $(S-4M_K^2)$ small. (b) $B_J^{(4)}(S) = \mathcal{O}(S^{-1})$ for large enough S , in particular for $S > 100M_K^2$. (c) $B_J^{(4)}(S)$ is an oscillating function of J ; in particular, it is positive for $J=0$, negative for $J=1$.

Property (a) is necessary, that we might use $B_J^{(4)}$ for the intended purpose of adjusting the value of $N_1(S)$ at threshold. Property (b) insures that the high-energy asymptotic behavior is governed by the Regge-pole exchange term, our fundamental input. Property (c) enables us to draw conclusions regarding the effect of $B_J^{(4)}$ on the Regge slopes and on the S -wave bound-state energies, without actually using $B_J^{(4)}$ in any of the integral equations except the one which determines the P -wave bound state; in particular only (3.12) has the additional term now $B_1^{(4)}(S)$. Numerical results, enabling us to see that effects in the other cases will be small, are discussed later.

IV. RELATIONSHIP OF MODEL TO STRIP APPROXIMATION

Chew, Frautschi, and Mandelstam²³ originally proposed a model for general two-body reactions; it was based on the iterative process for determining the elastic part of the double spectral functions in the Mandelstam representations, and the observation that over much of the energy range the nearest part (strip) of the spectral functions determined the main features of the amplitude, in particular for high energies and low-momentum transfers. No calculations based on this model in its complete form have been done, because of the severe numerical problems involved in handling the spectral functions for large values of their arguments, even after the question of subtractions was clarified¹⁰ by introducing Regge poles into the representation of the amplitude.

It was later proposed by Chew,¹⁵ and Chew and Jones,²⁵ that a good approximation to the strip approximation could be obtained by keeping only Regge poles in the crossed channels, ignoring the iterative construction of the spectral functions, and solving N/D equations for complex l to redetermine the Regge poles in a self-consistent manner. A portion of this problem in the $\pi\pi$ case was treated by Balazs²⁶ who obtained interesting numerical results, although he did not utilize Regge poles explicitly in the crossed channels.

This approximate version of the strip approximation is very close to the present model. There are essentially two points of departure. The first is that the equations written by Chew¹⁵ were cut off at some upper limit, this limit being treated as a free parameter in the computation of any given set of amplitudes; this insured that the high-energy limit of the amplitudes T_l would coincide

with the Born terms B_l , no matter what the latter were. In our model, we find that as a consequence of the fact that only Regge poles associated with vector mesons are introduced, the N_l functions always approach the B_l functions for sufficiently large S ; and we find that the D_l functions approach $+1$ for large positive S . (They are defined to do so only for large negative S .) Thus, the amplitudes in this model approach the Born terms, without the necessity of a cutoff.

The second point is our treatment of the P -waves threshold behavior, as discussed in the previous section. We have not written down a prescription for correcting the threshold behavior at higher l values, but it is clear that the procedure is capable of generalization to larger l by including higher order diagrams. This is closer to the original version of the strip approximation²³ than the procedure suggested by Chew.¹⁵ Although it is possible to formulate partial wave N/D equations which give the correct threshold behavior for $l=0$ and $l=1$, contain no divergence at large S , and contain no arbitrary parameters, following the approach of Chew,¹⁵ it is not possible to generalize them to $l > 1$ without introducing either a cutoff or new parameters. This is the reason the method outlined above is preferred by the author; the correction terms introduced in the above method may be directly correlated with properties of the double spectral functions for high mass contributions. For instance, a prescription for correcting the D -wave threshold may be constructed, by adding a sixth-order diagram and adjusting its amplitude, or adjusting another parameter in the fourth-order term used; and in each case we get a definite function of λ which can be used to compute the Regge trajectories.

One defect of the model is the omission of the Regge pole for Pomeranchukon (P) exchange, which is apparently important at least in high-energy nucleon-nucleon scattering.²⁷ Here, we simply assume that the bound-state properties are determined principally by the vector meson exchange, which means that the P -exchange effect is assumed to be small compared to the ρ exchange term for small t and not too large S .

If it is true that the contributions from higher order diagrams always have weaker asymptotic behavior than the vector meson Regge pole term, we have some hope that higher order diagrams do not disturb the bound-state characteristics which we compute from the one-pole diagram. This would be most likely to be true if the Regge trajectory of the exchanged meson has a small slope, so that $1-\alpha(0)$ is small. In the latter case, for a given coupling constant, the high-energy asymptotic behavior of N [in Eq. (2.9)] is the principal factor which determines the existence of a bound state, although the precise position and residue depend on the

²⁵ G. F. Chew and E. Jones, Lawrence Radiation Laboratory Report UCRL 10992 (to be published).

²⁶ L. A. P. Balazs, Phys. Rev. Letters **10**, 170 (1963); Phys. Rev. **132**, 867 (1963).

²⁷ For latest status of this concept, cf. A. Ahmadzadeh and I. A. Sakmar, Phys. Rev. Letters **11**, 439 (1963); K. J. Foley, S. J. Lindenbaum, W. A. Love, S. Dzaki, J. J. Russell, and L. C. Yuan, *ibid.* **11**, 425 (1963); Riazuddin and Fayyazuddin, Phys. Rev. **132**, 873 (1963).

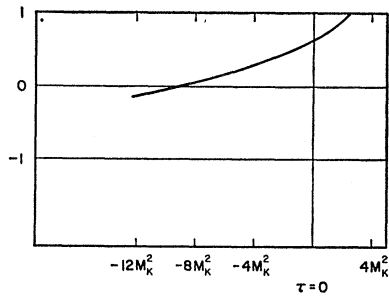


FIG. 3. Sketch of assumed $\alpha_\rho(t)$ for $\alpha'(M_\rho^2) = 0.25 M_K^{-2}$.

low-energy behavior of N . Since we can in turn compute the slope of a Regge trajectory associated with a bound state, and hence compute $\alpha(0)$ approximately if the slope is small, this is a favorable situation when applied to "bootstrap" calculations.

V. NUMERICAL RESULTS FOR THE $K\bar{K}$ MODEL

In the simple version of the model given here, we have two free "input" parameters, the $\rho K\bar{K}$ coupling constant and the Regge slope α' of the ρ meson trajectory. We assume that the detailed shape of the function $\alpha_\rho(t)$ is not important, and we use a two-pole representation

$$\alpha_\rho(t) = \alpha(-\infty) + \frac{R_1}{t_1 - t} + \frac{R_2}{t_2 - t}. \quad (5.1)$$

This form was suggested by the dispersion relation for²⁸ α and can represent quite accurately (for $t < 0$) trajectories known from the Schrödinger equation with a Yukawa potential.²⁹ We fix t_1 and t_2 at $4M_K^2$ and $8M_K^2$. The final results are quite insensitive to these values, as long as both t_1 and t_2 are greater than M_ρ^2 and not too close together. The asymptotic value $\alpha(-\infty)$ was chosen to be $-\frac{1}{2}$, in order to simulate the asymptotic behavior of the background integral of the Regge representation. The residues R_i were then fixed by the conditions $\alpha_\rho(M_\rho^2) = 1$ and $\alpha'_\rho(M_\rho^2) = \alpha'$, where α' is the free parameter. A typical trajectory $\alpha(t)$ is sketched in Fig. 3, for $\alpha' = 0.25 M_K^{-2}$. This value of α' corresponds approximately to the slope of trajectories originally suggested by Chew and Frautschi.³⁰ We investigate the solutions obtained for α' values between 0.12 and 0.50, where we take the K mass to be unity from now on.

The coupling constant parametrization in the numerical solutions is defined in terms of

$$\gamma \equiv 3f_\rho^2 / M_\rho^2. \quad (5.2)$$

For $\gamma \ll 1$, we get no bound states; for γ near unity, there is one S -wave bound state; then as γ reaches a

²⁸ J. R. Taylor, Phys. Rev. **127**, 2257 (1962); H. Cheng, *ibid.* **130**, 1283 (1963); A. Pignotti, Phys. Rev. Letters **10**, 416 (1963).

²⁹ A. Ahmadzadeh, P. G. Burke, and C. Tate, Phys. Rev. **131**, 1315 (1963); C. Lovelace and D. Masson, Nuovo Cimento **26**, 472 (1962).

³⁰ G. F. Chew and S. C. Frautschi, Phys. Rev. Letters **1**, 394 (1961); **8**, 41 (1962).

value between 5 and 10, there appears a P -wave resonance while the S -wave bound state moves lower in total energy. Values of γ greater than 15 were not investigated. The bound-state spectrum for specific values of γ and α' is exhibited in Fig. 4. The portion of the curves for $S_B < 0$ are intended to have only formal meaning.

We can relate γ to the vector coupling constant defined for an elementary vector meson. The amplitude from perturbation theory for the $T=0$ state of $K\bar{K}$, with the exchange of isovector ρ meson, would be

$$B_\rho^{(P)}(S, t) = -\frac{3 f_{\rho K K^2}}{4 \cdot 16\pi} \frac{S - \bar{S}}{M_\rho^2 - t}, \quad (5.3)$$

where $\bar{S} = 4M_K^2 - S - t$. Evaluating B_ρ from (2.2) for $\alpha = 1$ and large S , and comparing with (5.3) for large S , we get

$$\frac{f_{\rho K K^2}}{4\pi} = -\frac{4}{3} \left(\frac{4M_\rho^2}{4M_K^2 - M_\rho^2} \right) \gamma. \quad (5.4)$$

Substituting the numerical value for the mass $M_\rho = 1.58 M_K$, this relation becomes

$$f_{\rho K K^2} / 4\pi \cong 20\gamma. \quad (5.5)$$

Details of the methods used in numerical solution of our equations, using an electronic computer (IBM 7090), are discussed in the Appendix.

The computed Regge trajectory slopes behave as expected from potential theory; considering first the S -wave bound state, we find that for small binding energy the slope is very large and positive, and as the binding energy increases, the slope decreases. In the P -wave case, as the resonance first appears we find zero slope; then it becomes nonzero and positive. As the resonance moves down in energy after it becomes a bound state, the slope decreases again, but remains positive. These features can be recognized as following closely the behavior of $(-\partial D_l(S)/\partial S)$ at the bound

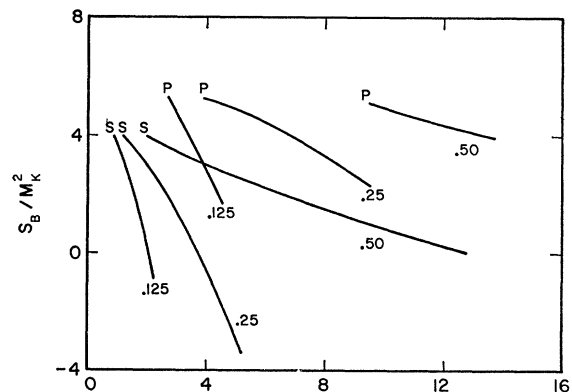


FIG. 4. Bound state and resonance energies, for various α'_ρ values, as a function of γ . S and P refer to $l=0$ and $l=1$, respectively. Values of α'_ρ indicated on graph.

state; the denominator of the expression (2.11) is found to be a slowly varying function of bound-state energy for both S and P waves, and remains positive for all cases examined, with a value for S waves always close to unity. Some numerical values for the computed slopes are given in Fig. 5, where a factor $(4M_K^2 - S_B)^{1/2}$ is introduced in the S -wave cases to get a nonsingular plot. The approximate trajectories, deduced from the $l=0$ and $l=1$ crossing points and slopes, are sketched in Fig. 6. The residues of the poles in $T_l(S)$ associated with the bound states were computed, and are given in Fig. 7. These residues are proportional to the square of the coupling constant of the bound state with $K\bar{K}$ system, the proportionality depending on the definition. We have tabulated the residues defined by

$$G_0^2 = \lim_{S \rightarrow S_B} \left(\frac{S - S_B}{M_K^2} \right) T_0(S) = \frac{N_0(S_B)}{M_K^2} \left[-\frac{d}{dS} \operatorname{Re} D_0(S) \right]_{S=S_B}^{-1} \quad (5.6)$$

for the S -wave bound states, and for the P waves (bound state or resonance)

$$G_1^2 = \frac{N_1(S_B)}{(S_B - 4M_K^2)} \left[-\frac{d}{dS} \operatorname{Re} D_1(S) \right]_{S=S_B}^{-1} \quad (5.7)$$

This definition is similar to (5.6) for $S_B < 4M_K^2$, and is continued for $S_B > 4M_K^2$ as suggested by Gell-Mann and Zachariasen.¹⁴

The residue G_1^2 determines the width of the φ meson as computed in our model. Explicitly, for $S_B = M_\varphi^2$, when $\operatorname{Re} D_1(S_B) = 0$, the full width (in energy units of the K mass) is

$$\Gamma_\varphi / M_K = G_1^2 (M_\varphi^2 - 4M_K^2)^{3/2} M_K / M_\varphi^2. \quad (5.8)$$

Typically, we find $G_1^2 \cong 2.5$ in our model when

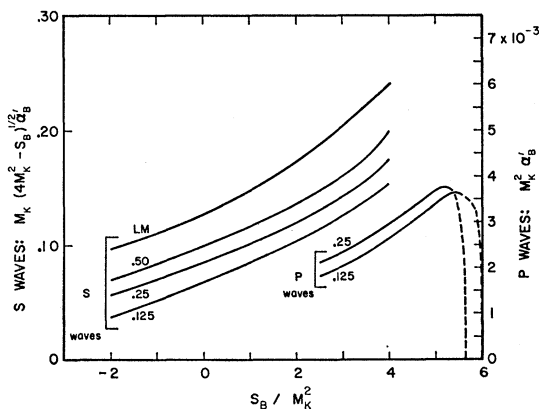


FIG. 5. Computed slope as a function of bound state energy, for various α' values (indicated on graph). Curve labeled LM is from Ref. 29, Lovelace and Masson. Note different scales for $l=0$ and $l=1$ cases.

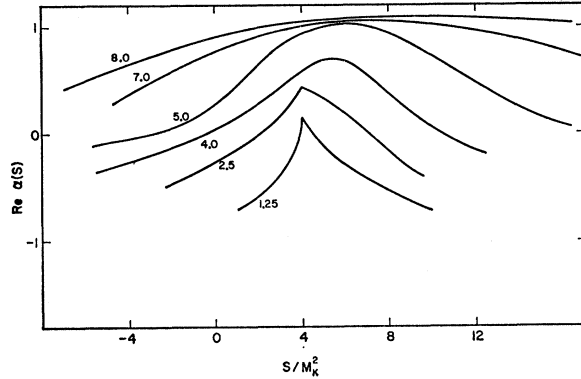


FIG. 6. Sketch of Regge trajectories for various values of γ , with $\alpha' = 0.25$, based on crossing points and slopes.

$\sqrt{S_B} = 1018$ MeV, for the best choices of γ and α' . This leads to $\Gamma_\varphi \cong 12$ MeV, a factor of 2 to 3 greater than the experimental data indicates. It should be remembered, however, that we have omitted the ω pole in the $T=0$ direct P -wave channel, and this may have an additional effect on the φ width. Furthermore, it is generally expected that a one-channel calculation usually yields resonance widths that are too wide, and the inclusion of higher mass channels (such as $N\bar{N}$ states) tends to narrow the width; see, for example, Capps.⁵ Thus, these results are encouraging, since we expect that further sophistication of the model will move the width closer to the experimental value.

It appears that an S -wave bound state σ of $K\bar{K}$ should exist in reality, if our model is at all significant. The energy of this bound state is quite sensitive to the assumed value of α' even if we determine parameter pairs (γ, α') resulting in the P -wave resonance at the experimental position. For most α' values investigated, the S -wave zero occurs at an unphysical energy $S_B < 0$; this probably would not happen if the bootstrap effect of σ exchange were included.

In reality, however, such a state would be strongly coupled to pions, and the decay or production of σ would exhibit a characteristic width of 200–300 MeV due to the S -wave decay $\sigma \rightarrow 2\pi$; here we assume the pion coupling comparable to the $K\bar{K}$ coupling for σ , and $M_\sigma \gg 2M_\pi$. Thus it would probably not be seen in effective mass plots. It is encouraging to note, however, that such a state fits well into the semiphenomenological analyses of nucleon-nucleon scattering,^{12,31} which employ pion resonances (or heavy mesons) as a source of the nucleon-nucleon potential. There might be a possibility of finding traces of σ as a contribution in intermediate states in reactions such as $K^- + P \rightarrow Y^* + \pi$, since such a particle would give unusual singularities in a box diagram.³²

³¹ R. A. Bryan, C. Dismukes, and N. Ramsay, Nucl. Phys. 45, 353 (1963); Riazuddin and Fayyazuddin, in Ref. 27.

³² I am indebted to Professor Christian Fronsdal for discussions on this point.

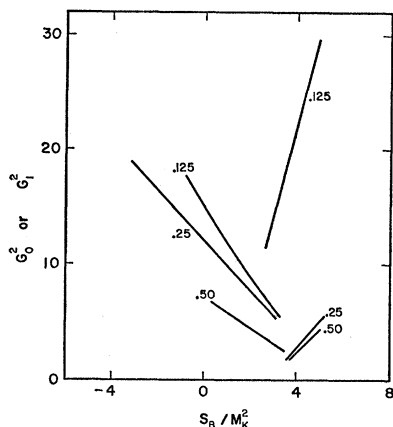


FIG. 7. Bound state residues G_0^2 and G_1^2 as defined in (5.6) and (5.7), for various α' values as indicated. The curves with positive slope are P -wave bound states and resonances, the others are S -wave bound states.

To return for a moment to the general properties of our solutions, one finds that when the contribution from $B_1^{(4)}(S)$ needed to establish correct threshold behavior in P -wave amplitudes has been fixed, it is found that adding the corresponding $B_0^{(4)}(S)$ (i.e., with the same g^2 value) to $B_0^{(0)}(S)$ changes the S -wave binding energies only a slight amount, of the order of 10% downwards in S_B . It is further found that $(\partial B^{(4)}(S)/\partial \lambda)$ evaluated at $\lambda=0$ and $\lambda=1$ is negligible compared to the ρ Regge-pole contribution; this is because $B_J^{(4)}$ is an oscillating function of J . Thus, the Regge slope calculations would be perturbed only slightly if we were to add the fourth-order terms in the slope equations. The corrections to F_1 have not been computed explicitly. It is necessary, however, to keep the complete expression [$B_1^{(0)} + B_1^{(4)}$] for the first term in (3.11), and everywhere in (3.9) and (3.10) where B_1 occurs, instead of (3.12).

We conclude this section by noting that Regge trajectory computations for bound states in the Schrödinger equation have been done with Yukawa potentials,²⁹ and we can compare our results for the Regge slopes of bound states with those calculations. Slopes were estimated from the graph given by Lovelace and Masson,²⁹ and those were plotted for comparison in Fig. 5. It is apparent that there is agreement to about 10% in the reduced slope values [slope multiplied by $(4M_K^2 - S_B)^{1/2}$] in the nonrelativistic region close to threshold, if we choose α' such that $\alpha(0)=0$, corresponding roughly to scalar meson exchange.

VI. DISCUSSION OF RESULTS; CONCLUSIONS

It can be seen from the numerical solutions that a few features of more crude approximations (e.g., the first-order determinantal method^{5,6}) are retained, and can be said to be "justified" in the framework of our model. The problem of a $K\bar{K}$ P -wave resonance has been treated using the older methods by Barbour and Nishimura,⁶ so

we have a reference point available for some of the numerical results of the present calculation.

The first point of favorable comparison is the determination of the width of the P -wave resonance. Our 12-MeV result (taking the smallest value obtained) for the one-channel approach coincides numerically with that of Ref. 6. This can be foreseen formally if the assumed Regge slope α' of the ρ is small enough; for in this case, a small value of coupling constant is required to give a P -wave resonance just above threshold, and the N_1 function is close to B_1 . It should be noticed that the computed resonance width is a ratio of the derivative of D to the value of N at the resonance position, and in the approximation $N=B$ the coupling constant cancels out. Thus, in the first-order determinantal method the resonance width is determined by kinematical factors such as the mass of the exchanged meson.

The second favorable comparison is in the adjustment necessary to achieve the proper P -wave threshold condition whenever N_1 differs appreciably from B_1 . Our model adds a term $B_1^{(4)}$ to the one-meson pole term, while as discussed earlier, other approaches are equivalent to adding a semiphenomenological far-away pole to the one-meson term. It is interesting to note, however, that our $B_1^{(4)}$ can be approximated rather well by a pole at $S=-40M_K^2$. Thus, the simpler approach gives essentially the same results, if one is only interested in the position and width of a P -wave resonance and does not try to compute Regge trajectory properties associated with such resonances.

On the other hand, since the bound state and resonance positions in our model are critically dependent upon the slope values α' , there is no justification of most of the various subtraction and cutoff procedures which have been used to get answers from vector-meson exchange terms. One cutoff procedure has been used by Scotti and Wong¹² which takes into account the existence of asymptotic behavior depending on α' ; cutoff in their model as well as ours comes about with factors of $S^{\alpha(0)-1}$. The form of the cutoff should not affect the low-energy scattering phase shifts, but it is certainly important in establishing the bound-state energies in our model. It should be noted that the Scotti and Wong form reduces to the perturbation theory expression at threshold, but this is not true in our model. There will be, then, at least a difference in the values required for coupling constants in a comparison of the bound-state properties between the two approaches.

The introduction of t_1 and t_2 as extra parameters in the trajectory may be avoided entirely by computing α_B'' and α_B''' as well as α_B' , through taking successive derivatives of (2.8) and (2.9), then solving the resulting integral equations, as done here for α_B' . If one wishes to go to this trouble, however, it would probably be simpler from the computation standpoint to solve (2.8) and (2.9) directly for a few noninteger values of λ selected to give a good representation of the trajectory $\alpha_B(t)$.

It is clear that the calculation done in the present work does not give any experimentally useful results, because (1) we cannot match the observed φ width by adjusting parameters, and (2) even if we get the φ mass correctly, the predicted σ meson mass is critically dependent on α' and is unphysical for a large range of α' . As mentioned previously, the latter problem might be cured by including the bootstrap effect of σ exchange, and the former by a multichannel calculation including $N\bar{N}$ states. Neither of these is certain, however, and such improved calculations should be done to check that improvements result. The numerical work presented was carried out not with any *a priori* belief in success in the physical system treated, but to illustrate that there are no hidden difficulties in applying the formalism, and get a start in seeing what Regge trajectories of such a model might look like. It is now hopeful that a straightforward application to the $N\bar{N}$ system will be interesting; one suspects that the π , η , ρ , and ω mesons will all have trajectories similar to those computed for S waves here, since they all may be treated as $l=0$ states in the $N\bar{N}$ system; and all of these would be put in as exchange terms analogous to (2.1) in the $K\bar{K}$ case.

It should be pointed out again that most of the physical ideas contained in the present work are not new^{33,15}; the emphasis on equations determining α' , and the numerical solutions, are contributed here.

ACKNOWLEDGMENTS

I would like to express my appreciation to Dr. Glen Culler and Dr. Burton Fried for assistance in preliminary investigations using the on-line computing center at Thompson-Ramo-Woolridge Corporation. The majority of the computation was carried out at the UCLA Computing Facility IBM 7090.

APPENDIX: DISCUSSION OF NUMERICAL SOLUTIONS FOR THE EQUATIONS

Here is an outline of the computation sequence used in the computer program for solving the S -wave equations. In each computation of a function, it is understood that 100 values of S were computed and stored.

- (1) $B_0(S)$ is computed; Eqs. (2.7), (2.4).
- (2) The integral equation (2.8), regarded as a matrix equation connecting 100 values of N_0 on each side, is inverted and the resolvent matrix stored.
- (3) $D_0(S)$, for 200 values of S (100 above and 100 below threshold) is computed by integrating [Eq. (2.9)] the solution N_0 .
- (4) $F_0(S)$ is computed [Eq. (2.15)]; then using F_0 and N_0 , G_0 is computed [Eq. (2.14)].
- (5) Equation (2.16) is solved, yielding 100 values of $E_0(S)$, by using the resolvent matrix obtained in step (2).

(6) The derivative (2.12) is computed for 200 S values, from the solutions N_0 and E_0 obtained in steps 1-6.

(7) The zeros of $D_0(S)$ are located, giving S_B , and at those positions the slope is evaluated through (2.11).

(8) Residues are computed, using Eq. (2.8) to compute values of N below threshold when required.

The 100-mesh point values of S were selected after much experimentation to give as good as possible a representation of the functions both near threshold, where rapid variations occur, and for large S values where it is important to retain the correct asymptotic behavior. Values out to $10^5 M_K^2$ were used. The integrals in (2.8), (2.9), (2.12), (2.13), and (2.14) were defined by Simpson's rule, as was the last term in (2.15) which also required 100 points. It is estimated that the over-all accuracy in most of the integrations is of order 10%, the error due largely to the high- S asymptotic region.

One of the advantages of the formulation given is that only one nonelementary function is required, $(\partial P_\lambda/\partial\lambda)_{\lambda=l}$, in addition to the basic Born term involving the P_α . Both the P_α occurring in (2.4) and the derivative $(\partial P_\lambda/\partial\lambda)_{\lambda=l}$ were evaluated using a 16-point Gaussian quadrature applied to the integral representation

$$P_\alpha(Z) = -\frac{1}{\pi} \int_0^\pi d\phi [Z + (Z^2 - 1)^{1/2} \cos\phi]^\alpha.$$

It was found, however, that in (2.4) the argument is always much larger than unity, and the asymptotic form Z^α could be used in (2.4) with an error of less than 10%. This was consistently done to speed up computing time.

It was also found that the second term in (2.4), as expressed in the third term in (2.15), and corresponding equations, contributed less than 5% to $F_0(S)$ and $F_1(S)$. This term was omitted for most of the calculations after the magnitude of this error was ascertained, again to speed up the computing process.

The fourth-order function $B^{(4)}$ required in the P -wave case was evaluated for $S < 10^3 M_K^2$ directly from (3.13), using 100-mesh points and Simpson's rule in each integral. For $S > 10^3 M_K^2$ the asymptotic behavior S^{-1} was found to hold and extrapolation was used from that point on.

The partial-wave projection integrals, and the first Z integration in (2.15), were done by 16-point Gaussian quadrature in Z for $S < 200 M_K^2$ and by 100-point Simpson's rule in t for $S > 200 M_K^2$. The representation was split up because the 16-point quadrature in Z did not give the correct asymptotic behavior, whereas the Simpson's rule method was not accurate enough for small values of S .

A complete set of S -wave solutions for each α' and γ , by steps 1-8 above, required 10 min of computing time on the 7090. The largest single tasks were step (2),

³³ Additional examples are: T. W. B. Kibble, Phys. Rev. **131**, 2282 (1963); Y. Miyamoto, Progr. Theoret. Phys. (Kyoto) **28**, 967 (1962); L. A. P. Balazs, Phys. Rev. **132**, 867 (1963).

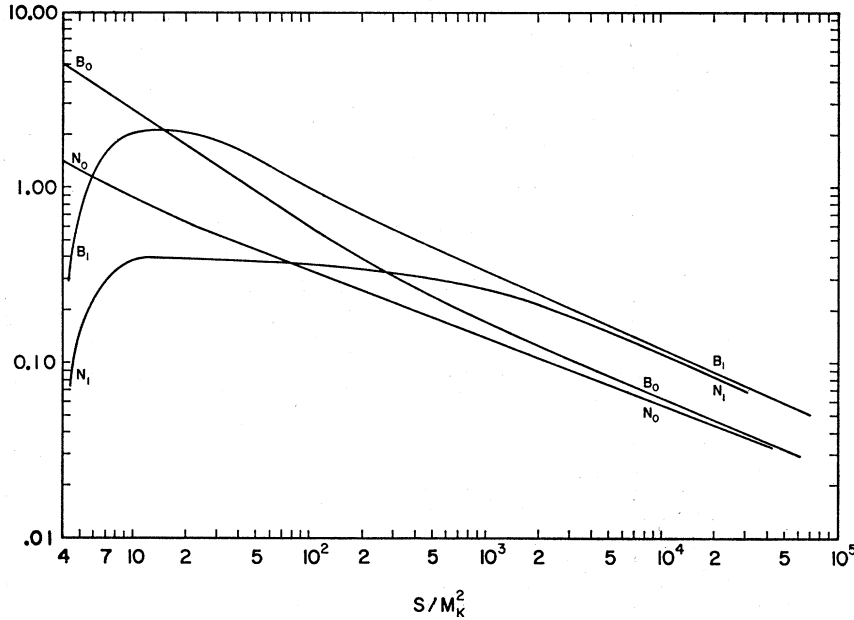


FIG. 8. B_0 and N_0 for $\alpha'=0.25$, $\gamma=2.5$; B_1 and N_1 for $\alpha'=0.25$, $\gamma=5.0$.

where inverting the 100×100 matrix used 2.5 min, and step (4) where computing F_0 required 5 min, when the approximations mentioned above were used. Without these approximations, the total computing time was increased by a factor of three.

The P -wave solutions used an average of 7 cycles through steps 1-2. After each cycle the threshold value of N_1 was examined, and a search program employed to vary g^4 [in (3.13)] until $N_1(4M_K^2)=0$ was achieved

with an accuracy ± 0.05 ; then steps 3-8 were executed as above. Total running time for a P -wave amplitude was about 30 min.

The time required for computing 100 values of $B_1^{(4)}$ was 20 min. This function was not recomputed each time since it does not depend on α' and γ ; values were stored on cards.

Some of the functions obtained in a typical set of solutions are given by Figs. 8 and 9. In Fig. 8 is plotted B_0 and N_0 for $\alpha'=0.25$, $\gamma=2.5$, and B_1 and N_1 for $\alpha'=0.25$, $\gamma=5.0$; in Fig. 9 we give $\text{Re}D_0$, $\text{Re}D_1$, $\text{Re}(\partial D_\lambda/\partial \lambda)_{\lambda=0}$, and $\text{Re}(\partial D_\lambda/\partial \lambda)_{\lambda=1}$ for the corresponding values of α' and γ . Here by B_1 we mean only the ρ pole term, whereas the N_1 solution given is that which is obtained after adding the proper $B_1^{(4)}$ contribution to B_1 as shown.

Finally, an approximation for $B_1^{(4)}$ was used which speeded up computing time for the P waves. After solutions were obtained using the function described in the text, it was found that $B_1^{(4)}$ could be approximated within 10% by a pole placed at $S = -40M_K^2$, and the solutions were essentially unchanged. This allowed replacing the trial-and-error computer program by an algebraic method for determining the appropriate residue, by writing a dispersion relation for $T_l(S)[(S+S_1)/(S-4M_K^2)]^l$ as described in Sec. III, where $S_1 = 40M_K^2$. This reduced the P -wave computation time to that of the S waves.

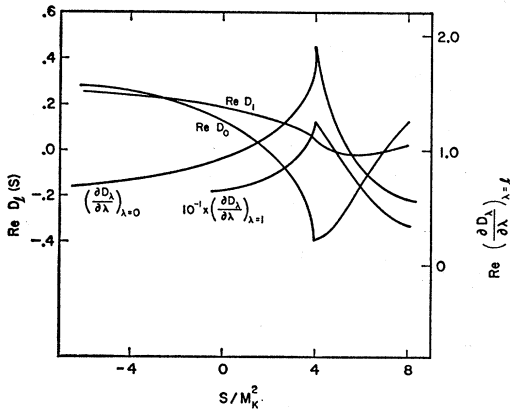


FIG. 9. $\text{Re}D_l(S)$ and $\text{Re}(\partial D_\lambda(S)/\partial \lambda)_{\lambda=l}$ for $l=0$ and $l=1$, parameter values corresponding to Fig. 8.